厚生労働科学研究費補助金（医療機器開発推進研究事業：ナノメディシン研究）
分担研究報告書

１１．造影超音波検査の現状と超音波分子イメージングへの期待

分担研究者　宮本幸夫　東京慈恵会医科大学　放射線科　准教授
協力研究者　中田典生　東京慈恵会医科大学　放射線科　講師

研究要旨：平成 18 年 1 月より第 2 世代超音波造影剤ソナゾイドによる肝臓腫瘍の診断が、臨床で実用化された。慈恵医大附属病院では、平成 19 年 3 月までに、約 200 例にソナゾイドによる超音波造影診断が施行され、その有用性が実証された。また、その延長上の超音波分子イメージングが、今後実用化される必要性、そして実現性が現実味をおびてきた。今回、北米放射線学会での造影超音波に関連した研究発表の動向を解析し、今後の超音波分子イメージングの方向性を考察した。

１．造影超音波を含む超音波検査の現状

画像診断領域における世界で最も規模の大きい学会である RSNA（北米放射線学会）のキーワード別の演題の 2001 年から 2005 年までの推移の集計結果を表 1 にまとめた。

RSNA(北米放射線学会)における
キーワード検索による演題数の年次推移

RSNA	CT	MDCT	MR	3T	Ultrasound	Sonography	PET	Total
2001	1881	15	899	2	181	89	69	4221
2002	2050	24	944	4	112	59	112	4318
2003	2181	44	924	7	182	49	157	4511
2004	2227	85	926	26	225	74	178	4609
2005	2361	144	895	24	217	75	214	4786

表 1　RSNA における演題数の推移

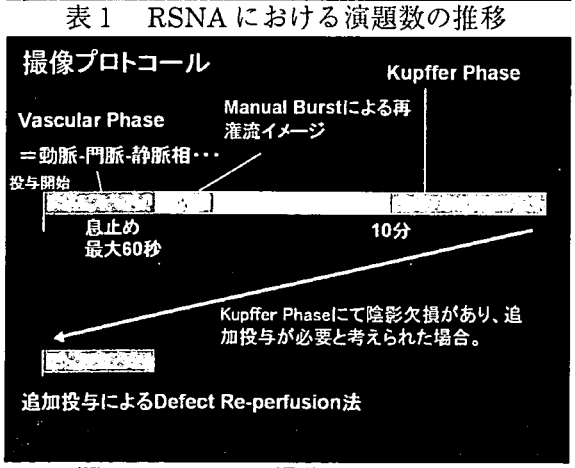

図 1　Sonazoid 撮像プロトコール

キーワード “Ultrasound” ないしは “Sonography”で検索される演題数はおおむね一定しており、“Ultrasound”で比較すると、全演題数の約 5 %程度で安定していることが分かる。この結果が示唆するように、超音波検査は米国においても一定の確立したモダリティであることがわかる。現在我が国の超音波造影剤は、第一世代である Levovist から第二世代の造影剤への移行過程にある。第二世代の造影剤とした現在 Sonazoid が認可されている。その平均直径は 2－4 μm のマイクロバブルであり、他のモダリティの造影剤に比べて平均径が多きく、造影剤の血管外漏出は基本的にない。2007 年 1 月に Sonazoid が認可されて以来、2008 年 3 月 21 日現在で 194 件の造影検査が東京慈恵会医科大学附属病院超音波診断センターにて施行されてきた。図 1 に当センターにおける Sonazoid 造影超音波検査の撮像プロトコールを記載する。図 2 にソナゾイドによる肝臓造影超音波検査の例として Hypervascular HCC の一例を示す。

２．造影超音波の新たな展望

今後の造影剤の新たな臨床適応について現在の動物実験などの研究[1)]を元にした推測をしてみる。超音波造影剤は経静脈投与のみならず、皮下注射によるリンパ管―リンパ節造影が期待されている。過去の研究を元に我々もブタによる実験を行った。この実験によると動物実験においては、センチネルリンパ節は良好に高輝度エコーとして造影されることが証明された。また経静脈投与では、腹部

実質臓器のみならず、表在領域の腫瘍の造影においても動物実験での有用性が示唆されている。このように現在使用されているマイクロバブルを用いた超音波造影剤の研究は、我々の進めているナノバブルの造影超音波の研究にも研究結果が反映されるものである。

3．超音波検査の将来と分子イメージング

一般に悪性腫瘍に接する血管内皮の細胞間隙は750nm以下である。そこで超音波造影剤の直径もなんとか750nm以下のナノバブルを作製して、かつ超音波像として画像化する必要がある。このようなサイズの小さい超音波造影剤が開発されると、CTやMRIと同様の造影像が得られる可能性がある[2]。また超音波造影剤の特徴として、音響薬理学的な特性として造影剤内の気泡に薬剤を封入することにより、ターゲットとなる部位で、強音圧の超音波を照射し、造影剤を破壊することにより、造影剤内の薬剤が放出されるというモデルがある。現在のマイクロバブルを用いた造影検査では、その解像度よりミリオーダーレベルの病変検出が限界である。しかしながら動物実験用の超高周波数の超音波検査装置では、探触子の周波数が25-75MHzで分解能が30μmである。これら周波数の高い探触子は、分解能は良好であるものの、焦点距離が短く体表からの深部臓器描出には限界がある[2]。近年、体内病変の検出に有効な内視鏡検査装置の進歩が著しい。内視鏡ロボットなどの開発も進んでいる。さらに超音波探触子の圧電素子をシリコンウエハー上に印刷し、マイクロオーダーの探触子の素子を製造することが可能となった。これらの技術革新により、近い将来体内の血管壁や病変部へ直接超音波探触子を挿入し、ナノバブル造影超音波検査を行って分子イメージングを施行するべくさらに技術革新を行う必要がある。

参考文献

1) Goldberg BB, Merton DA, Liu JB, Murphy G, Forsberg F. Contrast-enhanced sonographic imaging of lymphatic channels and sentinel lymph nodes. J Ultrasound Med. 2005 Jul;24(7):953-65.Click here to read

2) Rapoport N, Gao Z, Kennedy A. Multifunctional nanoparticles for combining ultrasonic tumor imaging and targeted chemotherapy. J Natl Cancer Inst. 2007 Jul 18;99(14):1095-106. Epub 2007 Jul 10.Click here to read

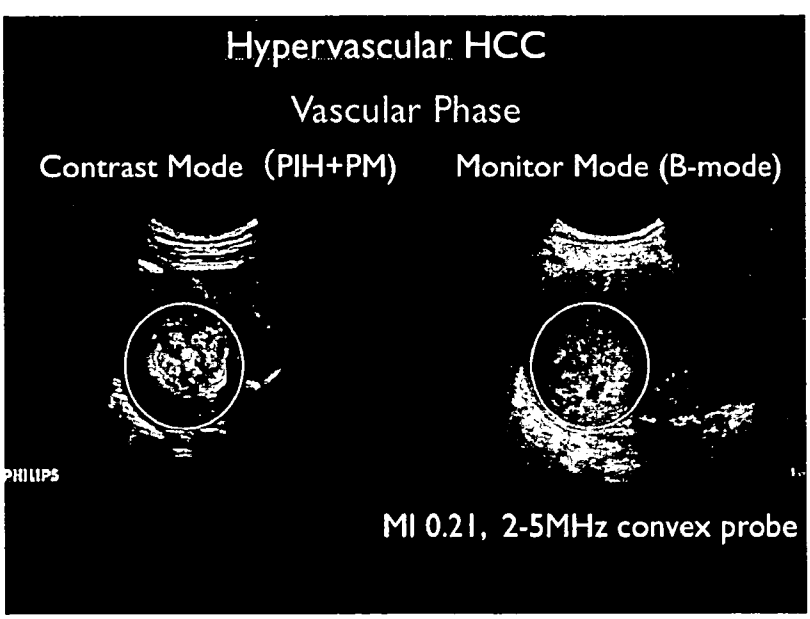

図2
ソナゾイド肝臓造影超音波像（Hypervascular HCC）。
図左側に投与約30秒後の造影早期から濃染する腫瘍染影が描出されている。図の右側は同一断面の通常のBモード像に描出されているやや淡い不均一な高エコーを呈するHCCが描出されている。

Ⅲ　研究成果の刊行に関する一覧表

研究成果の刊行に関する一覧表

書籍

著者氏名	論文タイトル名	書籍全体の編集者名	書　籍　名	出版社名	出版地	出版年	ページ

特になし

雑誌

発表者氏名	論文タイトル名	発表誌名	巻号	ページ	出版年
Eda H, Aoki K, Fujii K, Ohkawa K.	FGF-2 signaling induces downregulation of TAZ protein in osteoblastic MC3T3-E1 cells	***BBRC***	366	471-475	2008
Asakura T, Sasagawa A, Takeuchi H, Shibata S, Marushima H, Mamori S, Ohkawa K.	Conformational change in the active center region of GST P1-1 due to binding of a synthetic conjugate of DXR with GSH, enhanced JNK-mediated apoptosis	***Apoptosis***	DOI 10.1007		2007
Mamori T, Asakura T, Ohkawa K, Tajiri H.	Survivin expression in early hepatocellular carcinoma and post-treatment with anti-cancer drug under hypoxic culture	***World J Gastroenterol***	13(40)	1306-11	2007
Isome M, Lortie MJ, Murakami Y, Parisi E, Matsufuji S, Satriano J.	The antiproliferative effects of agmatine correlate with the rate of cellular proliferation.	***Am. J. Physiol. Cell Physiol.***	293(2)	C705-11	2007
Tanaka Y, Osaka T, Hattori A, Murakami Y, Matsufuji T, Matsufuji S, Shinkawa T, Isobe T, Mizutani T.	Soluble Liver Antigen/Liver and Pancreas, an Antigen in Autoimmune Hepatitis Patients: Influence on Selenocysteine Synthesis and its Complex with HSP70	***J. Health Sci.***	53(6)	682-691	2007
Tsukinaga S, Imazu H, Uchiyama Y, Kakutani H, Kuramochi A, Kato M, Tajiri H.	Diagnostic approach using endosonography guided fine needle aspiration for lymphadenopathy in primary sclerosing cholangitis	***World J Gastroenterol***	21	3758-9	2007
Mamori S, Nagatsuma K, Matsuura T, Ohkawa K, Hano H, Fukunaga M, Matsushima M, Masui Y, Fushiya N, Onoda H, Searashi Y, Takagi I, Tagiri H.	Useful detection of CD147 (EMMPRIN) for pathological diagnosis of early hepatocellular carcinoma in needle biopsy samples.	***World J Gastroenterol***	13(21)	2913-7	2007

Saito M, Matsuura T, Nagatsuma K, Tanaka K, Maehashi H, Shimizu K, Hataba Y, Kato F, Kashimori I, Tajiri H, Braet F.	The Functional Interrelationship between Gap Junctions and Fenestrae in Endothelial Cells of the Liver Organoid	***J Membr Biol.***	217	115-121	2007
Murakami K, Inoue Y, Hmwe SS, Omata K, Hongo T, Ishii K, Yoshizaki S, Aizaki H, Matsuura T, Shoji I, Miyamura T, Suzuki T.	Dynamic behavior of hepatitis C virus quasispecies in a long-term culture of the three-dimensional radial-flow bioreactor system.	***J Virol Methods.***	148(1-2)	174-81	2008
Omura N, Kashiwagi H, Yano F, Tsuboi K, Ishibashi Y, Kawasaki N, Suzuki Y, Mitsumori N, Urashima M, Yanaga K.	Prediction of recurrence after laparoscopic fundoplication for erosive reflux esophagitis based on anatomy-function-pathology (AFP) classification .	***Surg Endosc.***	21	427-30	2007
Ueda K, Yamada K, Urashima M, Ishibashi Y, Shirai M, Nikaido T, Takahashi H, Okamoto A, Saito M, Yasuda M, Ohkawa K, Tanaka T.	Association of extracellular matrix metalloproteinase inducer in endometrial carcinoma with patient outcomes and clinicopathogenesis using monoclonal antibody 12C3	***Oncol Rep.***	17	731-5	2007
Omura N, Kashiwagi H, Yano F, Tsuboi K, Ishibashi Y, Kawasaki N, Suzuki Y, Matsumoto A, Mitsumori N, Urashima M, Yanaga K.	Gastric ulcer after laparoscopic fundoplication for gastroesophageal reflux disease: significance of the eradication of Helicobacter pylori.	***Surg Laparosc Endosc Percutan Tech.***	17	193-6	2007
Nakayoshi T, Kawasaki N, Suzuki Y, Yasui Y, Nakada K, Ishibashi Y, Hanyu N, Urashima M, Yanaga K.	Epidural administration of morphine facilitates time of appearance of first gastric interdigestive migrating complex in dogs with paralytic ileus after open abdominal surgery.	***J Gastrointest Surg.***	11	648-54.	2007
Takakura S, Saito M, Ueda K, Motegi M, Takao M, Yamada K, Okamoto A, Niimi S, Sasaki H, Tanaka T, Ochiai K.	Irinotecan hydrochloride (CPT-11) and cisplatin as first-line chemotherapy after initial surgery for ovarian clear cell adenocarcinoma	***Int Surg.***	92	202-208	2007

Hashimoto H, Kusakabe M, and Ishikawa H,	A novel method for three-dimensional observation of the vascular networks in the whole mouse brain.	*Microsc Res Tech*	71(1)	51-9	2008
Ito T, Ohi S, Tachibana T, Takahara M, Hirabayashi T, Ishikawa H, Kusakabe M, and Hashimoto H	Development of the mucosal vascular system in the distal colon of the fetal mouse.	*Anat Rec*	291(1)	65-73	2008
Horiguchi Y, Yoshikawa A, Oribe K and Aizawa M.	Fabrication of Chelate-setting Hydroxyapatite Cements from Four Kinds of Commercially-available Powder with Various Shape and Crystallinity and Their Mechanical Property	*J. Ceram. Soc. Jpn.*	**116**	**50-55**	**2008**
Aizawa M, Ohno T, Kanomata N, Yano K and Emoto M.	Anti-tumorigenesis of Hollow Calcium-phosphate Microsphere Loaded with Anti-angiogenic Agent	*Key Engineer. Mater.*	361-363	1215-1218	2008
Aizawa M, Hiramoto A, Maehashi H, and Matsuura T.	Reconstruction of Liver Organoid Using an Apatite-fiber Scaffold, a Radial–flow Bioreactor, and FLC-4 Cells of Hepatocyte Model	*Key Engineer. Mater.*	361-363	1165-1168	2008
Sakai K, Umezawa S, Tamura M, Takamatsu Y, Tsuchiya K, Torigoe K, Ohkubo T, Yoshimura T, Esumi K, Sakai H, Abe M.	Adsorption and micellization behavior of novel gluconamide-type gemini surfactants.	*Colloid Interface Sci.*	318 (2)	440-448	2008
Abe M, Nakayama A, Kondo T, Morishita H, Tsuchiya K, Utsumi S, Ohkubo T, Sakai H.	Preparation of tiny biodegradable capsules using electrocapillary emulsification.	*J. Microencapsulation*	24 (8)	777-786	2007
Tsuchiya K, Ishikake J, Kim, T. S., Ohkubo T, Sakai H, Abe M.	Phase behavior of mixed solution of a glycerin-modified cationic surfactant and an anionic surfactant.	*J. Colloid Interface Sci.*	312 (1)	139-145	2007

Ⅳ　研究成果の刊行物・別刷

（別刷１２冊、日経産業新聞 2008年２月１日）

Association of extracellular matrix metalloproteinase inducer in endometrial carcinoma with patient outcomes and clinicopathogenesis using monoclonal antibody 12C3

KAZU UEDA[2], KYOSUKE YAMADA[2], MITSUYOSHI URASHIMA[1], YOSHIO ISHIBASHI[3], MISAKO SHIRAI[4], TAKASHI NIKAIDO[4], HIROYUKI TAKAHASHI[4], AIKOU OKAMOTO[2], MISATO SAITO[2], MAKOTO YASUDA[2], KIYOSHI OHKAWA[5] and TADAO TANAKA[2]

[1]Division of Clinical Research and Development; Departments of [2]Obstetrics and Gynecology, [3]Surgery, [4]Pathology and [5]Biochemistry, Jikei University School of Medicine, 3-25-8 Nishi-shinbashi, Minato-ku, Tokyo 105-8461, Japan

Received October 6, 2006; Accepted December 22, 2006

Abstract. Extracellular matrix metalloproteinase inducer (EMMPRIN) is a member of the immunoglobulin superfamily of adhesion molecules and has a role in the activation of several matrix metalloproteinases (MMPs). We evaluated whether EMMPRIN expression is related to tumor progression and patient outcome in human endometrial carcinoma. Paraffin-embedded surgical tissue samples from 112 patients with endometrial carcinoma were stained with anti-EMMPRIN antibody (monoclonal antibody 12C3:MoAb 12C3) for immunohistochemical analysis. EMMPRIN protein was expressed in cancerous lesions with the incidence of 97.3% (109 of 112 cases), but not in normal lesions. The scores determined by the combination of intensity and pattern of EMMPRIN staining in cancer cells correlated significantly with various histopathological risk factors: advanced stage, P=0.001; poorly differentiated carcinoma, P<0.001; lymph node metastasis, P=0.002; and lymphatic vessel infiltration, P=0.027. More importantly, recurrence-free survival was shortened in patients with higher EMMPRIN scores (HR, 3.08; 95% CI, 1.32-7.19; P=0.01). These results suggest that measurement of EMMPRIN expression with simple immunohistochemical staining may enhance the understanding of the pathophysiology of endometrial carcinoma.

Introduction

Matrix metalloproteinases (MMPs) are endopeptidases that play critical roles in promoting tumor disease progression, including tumor angiogenesis. In many solid tumors, MMP expression could be attributed to tumor stromal cells and is partially regulated by tumor-stroma interactions by means of tumor cell-associated extracellular matrix metalloproteinase inducer (EMMPRIN) (1). The roles of EMMPRIN and MMPs in tumor invasiveness have been confirmed immunohistochemically in several types of cancer cells (2-4). Moreover, research on EMMPRIN in malignant disease has recently attracted attention, and the expression of EMMPRIN has been reported to correlate with clinical prognosis of patients with breast carcinoma (5,6), ovarian carcinoma (7) and other types of cancer (8-11).

The prognosis for endometrial carcinoma patients with early clinical stage and well-differentiated carcinoma is generally satisfactory, but advanced stage and/or poorly differentiated carcinoma is an aggressive tumor with a poor prognosis (12-14). It would be beneficial to elucidate the pathophysiology of endometrial carcinoma concerning tumor invasiveness and differentiation.

We have established a murine monoclonal antibody (MoAb) 12C3 (15) that specifically binds to EMMPRIN protein (8). In the current study, EMMPRIN protein-expression patterns in endometrial carcinoma were examined immunohistochemically using MoAb 12C3 to determine their relation to clinicopathologic findings and recurrence-free survival.

Materials and methods

Tumor specimens. The Jikei University School of Medicine Ethics Review Committee approved the study protocol. A total of 112 endometrial carcinoma operative specimens were retrospectively obtained at the Jikei University Hospital (Tokyo, Japan) between January 1998 and March 2003. Tumors were histologically classified according to the WHO international system and the clinical cancer staging and the histological grade were defined according to the International Federation of Gynecology and Obstetrics (Table I). All of the 112 cases underwent hysterectomy, bilateral salpingo-oophorectomy and lymphadenectomy (or pelvic lymph node sampling). No cases received chemotherapy, radiotherapy or hormone therapy before they underwent operation.

Correspondence to: Dr T. Tanaka, Department of Obstetrics and Gynecology, Jikei University School of Medicine, 3-25-8 Nishi-shinbashi, Minato-ku, Tokyo 105-8461, Japan
E-mail: tanaka3520@jikei.ac.jp

Key words: EMMPRIN, endometrial carcinoma, monoclonal antibody, recurrence-free survival

Table I. Patient characteristics.

	n=112
Age (mean ± SD, years)	55.3±11.7
FIGO stage[a]	
I	68
II	18
III	21
IV	5
Histological type	
Endometrioid	101
Serous	4
Mucinous	1
Others	6

[a]The clinical cancer staging was defined according to the International Federation of Gynecology and Obstetrics.

Immunohistochemical analysis. For the immunohistochemical study, formalin-fixed paraffin-embedded sections were used. Immunostaining was performed using the labeled streptavidin-biotin peroxidase complex method with the Ventana auto-immunostaining system (Ventana Japan, Yokohama, Japan). A murine MoAb 12C3 against EMMPRIN protein was established as described (8). The antigen retrieval procedure was performed with a microwave oven in Dako antigen retrieval solution for 10 min at 95°C to efficiently stain the sample. The sections (Dako Cytomation, Glostrup, Denmark) were developed with 3,3'-diaminobenzidine with 0.3% H_2O_2 and counterstained with hematoxylin. As a negative control, pre-immune mouse serum diluted 100-fold with 1% bovine serum albumin (BSA; Sigma, St. Louis, MO) in 20 mM Tris-HCl, pH 7.6, 0.5 M NaCl (TBS) was used instead of MoAb.

Results of staining for EMMPRIN in cancerous lesions were evaluated using the following scoring system. The intensity of staining was classified into negative (0), weak (1), strong (2) or very strong (3), and the staining patterns were classified into negative (0), sporadic (1), focal (2) or diffuse (3), respectively and the total sum was evaluated. The examiners were blinded to patient clinicopathologic information when assigning staining intensity and patterns. Four investigators (K.U., K.Y., H.T. and M.U.) evaluated the staining results independently, after which discordant evaluations were adjusted by connected microscopes and scored finally.

Statistical analysis. χ^2 tests were used to evaluate the relationship between immunohistochemical scores and several clinicopathologic parameters. Survival curves of the patients were compared using the Kaplan-Meier method and analyzed by the log-rank test. Cox proportional hazard models were fitted for univariate and multivariate analysis. All these analyses were performed using STATA 8.0 (STATA Corp., College Station, TX).

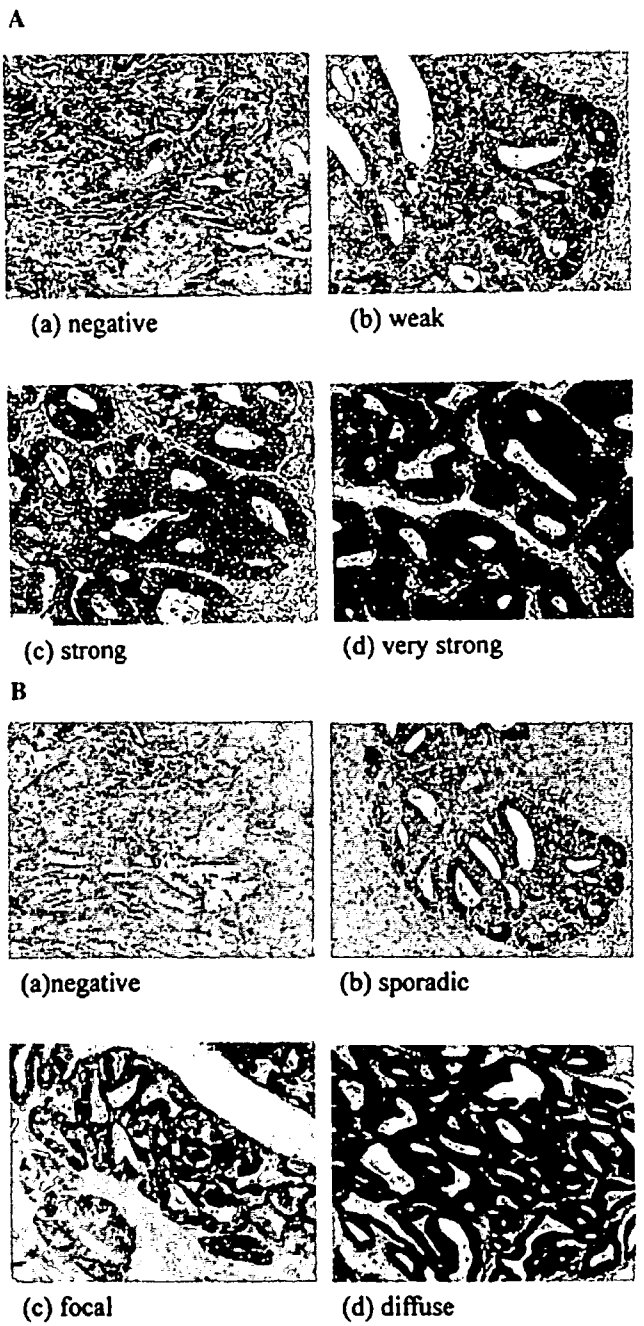

Figure 1. Immunohistochemical analysis and typical findings of EMMPRIN staining (intensity and pattern) in endometrial carcinoma using MoAb 12C3. EMMPRIN protein was expressed in cancerous lesions but not in normal lesions including the stromal cells and myometrium. (A) The intensity of staining was classified into negative (a), weak (b), strong (c), or very strong (d), respectively (magnification x200). (B) The staining patterns were classified into negative (a), sporadic (b), focal (c), or diffuse (d), respectively (magnification x100).

Results

Protein expression of EMMPRIN. MAb 12C3 reacted in 109 of 112 cases (97.3%) of endometrial carcinoma. EMMPRIN protein was expressed in cancerous lesions but not in normal lesions including the stromal cells and myometrium. Typical findings of EMMPRIN immunohistochemical staining (intensity and pattern) of paraffin-embedded specimens are

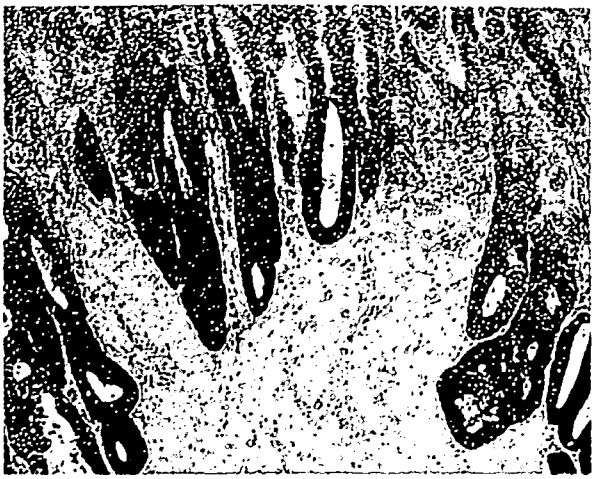

Figure 2. Immunohistochemical staining of endometrioid adenocarcinoma (Stage IIb, well-differentiated adenocarcinoma). EMMPRIN staining intensity was strong in deep cancer lesions with comparative examinations of serial tissue sections (magnification x100).

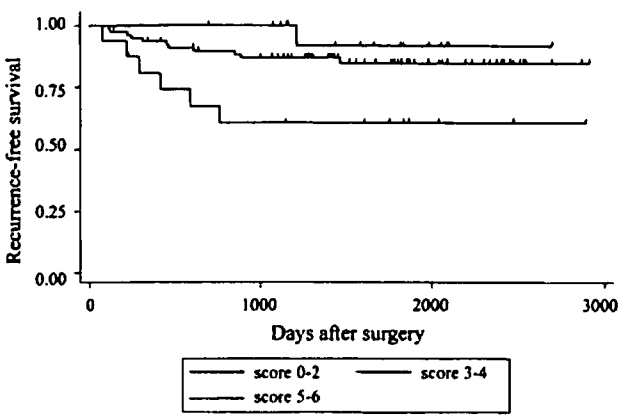

Figure 3. Kaplan-Meier survival curves by scores of EMMPRIN staining. Patients were grouped into three categories on expression of EMMPRIN: i) score 0-2; ii) score 3-4; iii) score 5-6. Statistical differences were analyzed with log-rank test (p=0.0153).

Table II. Clinicopathological characteristics of patients by scores of EMMPRIN staining.

	Score 0-2 (%)	Score 3-4 (%)	Score 5-6 (%)	P-value
Stage				0.001
I	15 (22)	50 (74)	3 (4)	
II	1 (6)	14 (78)	3 (17)	
III	1 (5)	12 (57)	8 (38)	
IV	0 (0)	3 (60)	2 (40)	
Grade				<0.001
1	16 (24)	46 (70)	4 (6)	
2	1 (3)	25 (81)	5 (16)	
3	0 (0)	6 (46)	7 (54)	
pN[a]				0.002
0	14 (17)	62 (76)	6 (7)	
1	1 (7)	8 (53)	6 (40)	
Lymphatic vessel infiltration				0.027
(-)	14 (23)	43 (70)	4 (7)	
(1+)	1 (4)	17 (68)	7 (28)	
(2+)	0 (0)	8 (73)	3 (27)	
(3+)	0 (0)	4 (80)	1 (20)	
Risk[b]				<0.001
Low	16 (24)	47 (70)	4 (6)	
High	1 (2)	32 (71)	12 (27)	
Recurrence				0.03
(-)	16 (17)	68 (72)	10 (11)	
(+)	1 (6)	11 (61)	6 (33)	

[a]0, no lymph node metastasis pathologically; 1, lymph node metastasis. [b]Low-risk patients: no deep myometrial invasion, no uterine cervical invasion and well-differentiated adenocarcinoma; high-risk patients, over stage Ic and/or poorly differentiated carcinoma.

demonstrated in Fig. 1. In some cases, the staining intensity tended to be strong in deep cancerous lesions compared to shallow lesions (Fig. 2).

Association between clinicopathogenesis and the scoring system. The association between clinicopathogenesis and immunohistochemical scores were evaluated (Table II). The scores reflecting the intensity and the pattern of EMMPRIN staining were significantly higher in advanced stage (P=0.001), poorly differentiated carcinoma (P<0.001), lymph node metastasis (P=0.002), lymphatic vessel infiltration (P=0.027), the pathological high-risk group (P<0.001) and patients with recurrence (P=0.03), respectively.

Survival analyses. Kaplan-Meier analysis on the subgroups of the scores (0-2, 3-4, 5-6) confirmed the prognostic impact in endometrial carcinoma (log-rank test, P=0.0153) (Fig. 3).

Cox hazard regression analyses were applied to determine the clinicopathological factors associated with recurrence-free survival using a univariate and multivariate manner (Table III). Univariate Cox regression analyses revealed that advanced stage, poorly differentiated carcinoma, lymph node metastasis, lymphatic vessel infiltration, and a high score group of immunohistochemical scoring were significant predictors of recurrence-free survival. On the other hand, multivariate Cox regression analysis showed advanced stage {hazard ratio, 1.16 [95% confidence interval (CI), 1.08-1.25]} and poorly differentiated carcinoma [hazard ratio, 2.35 (95% CI, 1.00-2)] were the only significant poor prognostic factors.

Discussion

In this study, we determined protein expression of EMMPRIN in cancer cells with immunohistochemical staining, and

Table III. Univariable and multivariable analyses of factors associated with recurrence-free survival.

	Univariable analysis HR (95% CI)	P-value	Multivariable analysis HR (95% CI)	P-value
Score	3.08 (1.32-7.19)	0.01	0.53 (0.06-4.45)	0.557
Stage	1.14 (1.08-1.19)	<0.001	1.16 (1.08-1.25)	<0.001
Grade	3.63 (1.98-6.66)	<0.001	2.35 (1.00-5.50)	0.049
Risk	14.67 (3.36-63.93)	<0.001	0.03 (0.0001-6.54)	0.199
pN	15.26 (5.18-44.95)	<0.001	0.19 (0.01-5.28)	0.326
pM[a]	7.82 (2.22-27.)	0.001	0.08 (0.002-3.13)	0.175
Positive ascites[b]	5.53 (2.14-14.32)	<0.001	1.14 (0.22-5.83)	0.871
Lymphatic vessel infiltration	4.52 (2.66-7.69)	<0.001	2.32 (0.81-6.63)	0.117

[a]Distant metastasis. [b]Cancer cells in ascites or peritoneal washings.

investigated the association of this protein expression with clinicopathologic findings and recurrence-free survival in 112 patients with endometrial carcinoma. EMMPRIN protein was detected in cancerous lesions but not in normal lesions including the stromal cells and myometrium. Generally, the prognosis of low-risk patients with no deep myometrial invasion, no uterine cervical invasion and well-differentiated adenocarcinoma is satisfactory (16-18). EMMPRIN expression was confirmed not only in high-risk patients with higher stage (over stage Ic) and/or poorly differentiated carcinoma but also in lower risk patients. However, the scores reflecting the intensity and the pattern of EMMPRIN staining in cancer cells were significantly higher in high-risk patients, especially those with advanced stage, poorly differentiated carcinoma, lymph node metastasis, and lymphatic vessel infiltration. The staining scores were associated with recurrence-free survival and seemed to parallel clinical stage. Among stage I cases, although the staining scores were not associated with depth of myometrial invasion statistically, it was notable that the staining intensity was strong in deep cancerous lesions with comparative examinations of serial tissue sections. These results suggested that measurement of EMMPRIN expression with simple immunohistochemical staining might further enhance the understanding of the pathophysiology of endometrial carcinoma.

In clinical treatment, it is important to accurately diagnose surgical staging of endometrial carcinoma by performing systematic lymphadenectomy in addition to hysterectomy, and bilateral salpingo-oophorectomy for decisions concerning adjuvant chemotherapy. However, it is still controversial whether systematic lymphadenectomy can be omitted from remedies for low-risk patients with no deep myometrial invasion and well-differentiated adenocarcinoma. Usually pre-operative evaluation of endometrial carcinoma is mainly performed by D&C (dilation and curettage) and imaging including ultrasonography and MRI (magnetic resonance imaging), but there is a limit to this procedure in terms of identification of low-risk cases. We were able to validate the clinical importance of EMMPRIN expression retrospectively using 112 clinical paraffin-embedded specimens. In the current study, while we have not evaluated EMMPRIN expression using pre-operative endometrial materials, the measurement of EMMPRIN may serve as an additional tool for endometrial carcinoma diagnosis including pre-operative evaluation.

MMP expression has been demonstrated to be associated with cancer infiltration and invasion into vessels, suggesting that MMP inhibitors may prolong recurrence-free survival by interfering with tumor infiltration and invasion. In endometrial carcinoma, MMP-7, a member of the MMP family, has been reported to be associated with invasiveness, metastatic spread and poor prognosis (19). Recently, research of EMMPRIN in malignant disease has increased and the expression of EMMPRIN has been reported to correlate with clinical prognosis of patients with several malignancies. It has been reported that expression of EMMPRIN protects cancer cells from anoikis through inhibition of Bim (20). However, the molecular mechanisms underlying the actions of EMMPRIN and relation to MMPs are not fully understood, and no report has demonstrated blockade of EMMPRIN molecules in malignant diseases.

As a future direction, MoAb 12C3 may also be useful as a targeting agent for cancer imaging and/or chemotherapy. Further investigations are necessary to elucidate EMMPRIN's function including its relationship with MMP expression in endometrial carcinoma.

Acknowledgements

This study was supported by Grant-in-Aid for Scientific Research, Japan (no. 16659455).

References

1. Tang Y, Nakada MT, Kesavan P, McCabe F, Millar H, Rafferty P, Bugelski P and Yan L: Extracellular matrix metalloproteinase inducer stimulates tumor angiogenesis by elevating vascular endothelial cell growth factor and matrix metalloproteinases. Cancer Res 65: 3193-3199, 2005.
2. Kanekura T, Chen X and Kanzaki T: Basigin (CD147) is expressed on melanoma cells and induces tumor cell invasion by stimulating production of matrix metalloproteinases by fibroblasts. Int J Cancer 99: 520-528, 2002.

3. Marionnet C, Lalou C, Mollier K, Chazal M, Delestaing G, Compan D, Verola O, Vilmer C, Cuminet J, Dubertret L and Basset-Seguin N: Differential molecular profiling between skin carcinomas reveals four newly reported genes potentially implicated in squamous cell carcinoma development. Oncogene 22: 3500-3505, 2003.
4. Sier CF, Zuidwijk K, Zijlmans HJ, Hanemaaijer R, Mulder-Stapel AA, Prins FA, Dreef EJ, Kenter GG, Fleuren GJ and Gorter A: EMMPRIN-induced MMP-2 activation cascade in human cervical squamous cell carcinoma. Int J Cancer 118: 2991-2998, 2006.
5. Davidson B, Konstantinovsky S, Nielsen S, Dong HP, Berner A, Vyberg M and Reich R: Altered expression of metastasis-associated and regulatory molecules in effusions from breast cancer patients: a novel model for tumor progression. Clin Cancer Res 10: 7335-7346, 2004.
6. Reimers N, Zafrakas K, Assmann V, Egen C, Riethdorf L, Riethdorf S, Berger J, Ebel S, Janicke F, Sauter G and Pantel K: Expression of extracellular matrix metalloproteases inducer on micrometastatic and primary mammary carcinoma cells. Clin Cancer Res 10: 3422-3428, 2004.
7. Davidson B, Goldberg I, Berner A, Kristensen GB and Reich R: EMMPRIN (extracellular matrix metalloproteinase inducer) is a novel marker of poor outcome in serous ovarian carcinoma. Clin Exp Metastasis 20: 161-169, 2003.
8. Ishibashi Y, Matsumoto T, Niwa M, Suzuki Y, Omura N, Hanyu N, Nakada K, Yanaga K, Yamada K, Ohkawa K, Kawakami M and Urashima M: CD147 and matrix metalloproteinase-2 protein expression as significant prognostic factors in esophageal squamous cell carcinoma. Cancer 101: 1994-2000, 2004.
9. Jin JS, Hsieh DS, Lin YF, Wang JY, Sheu LF and Lee WH: Increasing expression of extracellular matrix metalloprotease inducer in renal cell carcinoma: tissue microarray analysis of immunostaining score with clinicopathological parameters. Int J Urol 13: 573-580, 2006.
10. Rosenthal EL, Shreenivas S, Peters GE, Grizzle WE, Desmond R and Gladson CL: Expression of extracellular matrix metalloprotease inducer in laryngeal squamous cell carcinoma. Laryngoscope 113: 1406-1410, 2003.
11. Zheng H, Takahashi H, Murai Y, Cui Z, Nomoto K, Miwa S, Tsuneyama K and Takano Y: Pathobiological characteristics of intestinal- and diffuse-type gastric carcinoma in Japan: an immunostaining study on the tissue microarray. J Clin Pathol (In press).
12. Lax SF, Kurman RJ, Pizer ES, Wu L and Ronnett BM: A binary architectural grading system for uterine endometrial endometrioid carcinoma has superior reproducibility compared with FIGO grading and identifies subsets of advance-stage tumors with favorable and unfavorable prognosis. Am J Surg Pathol 24: 1201-1208, 2000.
13. Lurain JR: Uterine cancer. In: Novak's Gynecology. 13th edition. Berek JS (ed). Lippincott Williams & Wilkins, Philadelphia, PA, USA, pp1143-1197, 2002.
14. Zaino RJ, Kurman RJ, Diana KL and Morrow CP: The utility of the revised International Federation of Gynecology and Obstetrics histologic grading of endometrial adenocarcinoma using a defined nuclear grading system. A Gynecologic Oncology Group study. Cancer 75: 81-86, 1995.
15. Yamada K, Ohkawa K and Joh K: Monoclonal antibody, Mat 12C3, is a sensitive immunohistochemical marker of early malignant change in epithelial ovarian tumor. Am J Clin Patho 103: 288-294, 1995.
16. Morrow CP, Bundy BN, Kurman RJ, Creasman WT, Heller F Homesley HD and Graham JE: Relationship between surgical pathological risk factors and outcome in clinical stage I and I carcinoma of the endometrium: a Gynecologic Oncology Grou study. Gynecol Oncol 40: 55-65, 1991.
17. Murray SK, Young RH and Scully RE: Unusual epithelial an stromal changes in myoinvasive endometrioid adenocarcinom a study of their frequency, associated diagnostic problems, ar prognostic significance. Int J Gynecol Pathol 22: 324-33 2003.
18. Nordstrom B, Bergstrom R and Strang P: Prognostic ind models in stage I and II endometrial carcinoma. Anticancer R 18: 3717-3724, 1998.
19. Misugi F, Sumi T, Okamoto E, Nobeyama H, Hattori Yoshida H, Matsumoto Y, Yasui T, Honda K and Ishiko Expression of matrix metalloproteinases and tissue inhibitors metalloproteinase in uterine endometrial carcinoma an correlation between expression of matrix metalloproteinas and prognosis. Int J Mol Med 16: 541-546, 2005.
20. Yang JM, O'Neill P, Jin W, Foty R, Medina DJ, Xu Z, Lomas Arndt GM, Tang Y, Nakada M, Yan L and Hait WN: Ex cellular matrix metalloproteinase inducer (CD147) conf resistance of breast cancer cells to Anoikis through inhibitio Bim. J Biol Chem 281: 9719-9727, 2006.

J Membrane Biol (2007) 217:115–121
DOI 10.1007/s00232-007-9022-3

The Functional Interrelationship between Gap Junctions and Fenestrae in Endothelial Cells of the Liver Organoid

Masaya Saito · Tomokazu Matsuura · Keisuke Nagatsuma · Ken Tanaka · Haruka Maehashi · Keiko Shimizu · Yoshiaki Hataba · Fumitaka Kato · Isao Kashimori · Hisao Tajiri · Filip Braet

Received: 28 March 2007 / Accepted: 4 April 2007 / Published online: 14 June 2007

Abstract Functional intact liver organoid can be reconstructed in a radial-flow bioreactor when human hepatocellular carcinoma (FLC-5), mouse immortalized sinusoidal endothelial M1 (SEC) and A7 (HSC) hepatic stellate cell lines are cocultured. The structural and functional characteristics of the reconstructed organoid closely resemble the *in vivo* liver situation. Previous liver organoid studies indicated that cell-to-cell communications might be an important factor for the functional and structural integrity of the reconstructed organoid, including the expression of fenestrae. Therefore, we examined the possible relationship between functional intact gap junctional intercellular communication (GJIC) and fenestrae dynamics in M1-SEC cells. The fine morphology of liver organoid was studied in the presence of (1) irsogladine maleate (IM), (2) oleamide and (3) oleamide followed by IM treatment. Fine ultrastructural changes were studied by transmission electron microscopy (TEM) and scanning electron microscopy (SEM) and compared with control liver organoid data. TEM revealed that oleamide affected the integrity of cell-to-cell contacts predominantly in FLC-5 hepatocytes. SEM observation showed the presence of fenestrae on M1-SEC cells; however, oleamide inhibited fenestrae expression on the surface of endothelial cells. Interestingly, fenestrae reappeared when IM was added after initial oleamide exposure. GJIC mediates the number of fenestrae in endothelial cells of the liver organoid.

Keywords Electron Microscopy · Defenestration · Fenestra · Fenestrae formation · Liver sieve · Pore · Porosity · Sinusoidal endothelial cell · Transendothelial channel · Transendothelial transport

M. Saito (✉) · T. Matsuura · K. Nagatsuma · K. Tanaka · H. Tajiri
Division of Gastroenterology and Hepatology, Department of Internal Medicine, Jikei University School of Medicine, 3-25-8 Nishi-shinbashi, Minato-ku Tokyo 105-8461, Japan
e-mail: masayas@jikei.ac.jp

T. Matsuura
Department of Laboratory Medicine, Jikei University School of Medicine, Tokyo, Japan

H. Maehashi · K. Shimizu
Department of Biochemistry I, Jikei University School of Medicine, Tokyo, Japan

Y. Hataba
Integrated Imaging Research Support, Tokyo, Japan

F. Kato · I. Kashimori
Pharmacology Research Group, Discovery Research Laboratories, Nippon Shinyaku, Kyoto, Japan

F. Braet
Australian Key Centre for Microscopy and Microanalysis, University of Sydney, Sydney, NSW 2006, Australia

Introduction

Previously, we reported that functional liver organoid was able to reassemble when human hepatocellular carcinoma cells (FLC-5), mouse immortalized sinusoidal endothelial cells (M1-SEC) and mouse immortalized hepatic stellate cells (A7 HSC) were cocultured in a radial-flow bioreactor (RFB). The intricate structural arrangement of the reconstructed liver organoid was proven to be successful as urea production in function of time could be measured as a biochemical functional marker in the supernatant. Furthermore, fenestrae were clearly detected as a structural indicator on the surface of M1-SEC cells (Saito et al.,

2006). We postulated at that time that cell-to-cell communications were an important factor in the successful reconstruction of a functional liver organoid in the RFB.

Gap junctional intercellular communication (GJIC) is one of the family members of junctional complex systems that allow transport of low-molecular weight molecules such as ions and second messengers. GJIC complexes also have an important role in regulating cell growth and tissue homeostasis (Evans & Martin, 2002). Several studies on vascular endothelial cells have shown that gap junctions between the cellular layers of arteries have important roles for altering the phenotype of endothelial cells and regulating the vascular diameter (de Wit, Hoepfl & Wolfle, 2006; Rummery & Hill, 2004; van Veen, van Rijen & Jongsma, 2006). However, to date, there is no evidence available describing the relation between SEC fenestrae and gap junctions.

Liver sinusoidal endothelial fenestrae have been shown to be responsive under numerous physiological (Wisse et al., 1985) and pathophysiological (Fraser, Dobbs & Rogers, 1995) conditions, including various pharmaceutical compounds (Braet & Wisse, 2002). The function of these peculiar membrane-bound holes which lack any diaphragm has been demonstrated in several relevant medical conditions such as cirrhosis, lipid transport and blood flow regulation (Oda, Han & Nakamura, 2000). In brief, these open pores act as bidirectional guardians for regulating the transendothelial transport of solutes, particles and food substances between the liver sinusoidal blood and the hepatocytes (Wisse, 1970).

In recent times, special attention has been paid to learning more about the origin (fenestrae formation) and loss (defenestration) of liver sinusoidal endothelial fenestrae (Braet, 2004). More recently, similar mechanisms in the dynamics and formation of diaphragmed fenestrae have been described in an endothelioma cell line (Ioannidou et al., 2006); and in the liver sinusoidal field, it was demonstrated that endothelial fenestrae could be induced in M1-SEC cells (Saito et al., 2004) and primary cultured SEC cells (Braet et al., 1998, 2007) using anti-actin agents. At present, the majority of fenestral studies are focused on finding ways to increase the liver sieve's porosity by pharmaceutical means (Braet et al., 2004; Yokomori et al., 2004). By doing so, one may hope to restore the normal liver sieving function in humans suffering from one or another fenestrae-related disorder (Braet, 2004).

In the present study, we examined the effects of the pharmaceutical compounds irsogladine maleate (IM) and oleamide on the ultrastructure and numerical dynamics of endothelial fenestrae of M1-SEC cells cultured in the RFB. IM and its antagonist oleamide have been reported to influence gap junctional function in epithelial and endothelial cells (Uchida et al., 2005; Nakashima et al., 2000; Inoguchi et al., 1995). Furthermore, there is mounting preliminary evidence illustrating the interrelation between functional gap-junctional complexes and various transendothelially mediated processes (Zahler et al., 2003; Feng et al., 1997).

The aims of our study were therefore to explore (1) the possible functional relationship between GJIC and hepatic fenestrae and (2) whether functional GJIC can induce fenestrae in endothelial cells of the liver organoid.

Materials and Methods

Cell Culture

In this study, we used a functional human hepatocellular carcinoma cell line (FLC-5) known to express drug metabolism enzymes (e.g., human-type carboxyl esterase or cytochrome) and liver-specific proteins such as albumin. *In vitro*, this cell line retains its capability for three-dimensional reorganization and possesses distinct microvilli on the cell surface. As a nonparenchymal endothelial cell line we used the immortalized M1-SEC line (Matsuura et al., 1998). The immortalized HSC line A7 (Matsuura et al., 1999) was established by isolating nonparenchymal cells from an H-2Kb-tsA58 transgenic mouse liver transfected with the simian virus 40 large T antigen gene (Jat et al., 1991). Cocultures of FLC-5, M1 and A7 cells were grown in ASF104 medium enriched with 2% fetal bovine serum.

Drug Compounds

IM [2,4-diamino-6-(2, 5-dichlorophenyl)-striazine maleate], an antiulcer drug which increases the activity of GJIC complexes via the cyclic adenosine monophosphate (cAMP) pathway, was obtained from Nippon Shinyaku (Kyoto, Japan). Oleamide is a sleep-inducing drug for animal purposes that inhibits GJIC function and was purchased from Sigma (St. Louis, MO).

Electron Microscopy

Fine structural changes were observed by means of transmission electron microscopy (TEM) and scanning electron microscopy (SEM).

For TEM, cultured cells were fixed with 2% glutaraldehyde in 0.1 M phosphate buffer (PB) for 1 h and post-fixed with 1% OsO_4 in 0.1 M PB for 1 h at 4°C. Specimens were dehydrated in ethanol and subsequently embedded in a mixture of Epon-araldite. Thin sections (60 nm) were cut with a diamond knife mounted on an LKB (Bromma, Sweden) ultratome and stained with aqueous uranyl ace-

tate. Specimens were examined with a JEOL (Tokyo, Japan) 1200EX electron microscope at 80 kV.

For SEM, cultured cells were fixed with 1.2% glutaraldehyde in 0.1 M PB at pH 7.4 and postfixed with 1% OsO_4 in 0.1 M PB. The fixed cells were rinsed twice with phosphate-buffered saline, subsequently dehydrated in ascending concentrations of ethanol, critical point-dried using carbon dioxide and coated by vacuum-evaporated carbon and ion-sputtered gold. Specimens were observed using a JSM-35 (JEOL) at an accelerated voltage of 10 kV.

Monolayer Culture Experiments of M1 Cells

Confluent dishes of M1 cells were cultured in ASF 104 medium with or without 10 μM IM for 3 days. IM was replaced every 24 h. Fine morphology of fenestrae of M1 cells was observed by SEM. For immunofluorescence studies, a rabbit polyclonal antibody directed against a 23-amino acid C-terminal peptide sequence within the cytoplasmic domain of mouse Cx43 (Chemicon, Temecula, CA; AB1728) was used at a 1:500 dilution in 0.1 M PB. Alexa Fluor 488-conjugated goat anti-rabbit immunoglobulin G (Molecular Probes, Eugene, OR; A-11008) was used as secondary antibody and diluted 1:1,000 in 0.1 M PB containing 1:200 goat serum. Next, dishes were washed three times in PB for 5 min. Samples were examined with an LSM 510 confocal laser scanning microscope (Carl Zeiss, Oberkochen, Germany).

RFB Cocultures

FLC-5 cells (1×10^7) were seeded in the RFB. After 5 days, 1×10^7 A7 cells were added in a similar manner, followed by another addition of 5×10^6 M1 cells 5 days later. Next, the cell line cocultures were allowed to culture for an additional 3 days to permit liver organoid reconstruction in the RFB as described (Saito et al., 2006). The RFB system used in this study is made of a 5-ml radial-flow chamber, a mass flow controller and a closed circuit reservoir (RA-5; ABLE, Tokyo, Japan). Culture medium was changed manually to maintain optimal glucose, lactate and pH levels (Saito et al., 2006).

IM and Oleamide Drug Treatment

The fine morphology of liver organoid was studied in the presence of (1) IM, (2) oleamide and (3) oleamide followed by IM treatment. More specifically, 10 μM IM was added every 24 h from day 14 until day 16. Oleamide (100 μM) was added every 24 h from day 13 until day 14. For the combined treatment, oleamide was added in a similar manner as outlined above, followed by another addition of 10 μM IM for 2 days.

Subsequently, samples were prepared for electron microscopy as outlined above, and fine ultrastructural changes were studied by TEM and SEM. Treated samples were compared with control monolayers and/or liver organoid data.

Results

In monolayers of M1 cells, the presence of connexin 43 was confirmed by confocal microscopy. A distinct positive staining for connexin 43 in the form of dots could be observed at the cell-cell contact sites (Fig. 1). SEM investigation of M1-treated cells showed an increased number of small pores resembling coated pits when treated with IM (Fig. 2).

TEM observation of the reconstructed liver organoid showed that cultured cells form multiple layers of cells mimicking liver tissue organization. The cells are closely interconnected with the neighboring cells in both control (Fig. 3a) and IM (Fig. 3b) conditions. Intercellular junctions are clearly present and keep the cells together as in the liver tissue context.

When the liver organoid was exposed to oleamide, the number of cell-to-cell contacts was overall significantly reduced,but loss was more pronounced in the areas where FLC-5 hepatocytes reside (Fig. 3c). Additionally, an overall loss in tissue architecture of the liver organoid could be observed and, instead, large clefts between the individual cells became apparent.

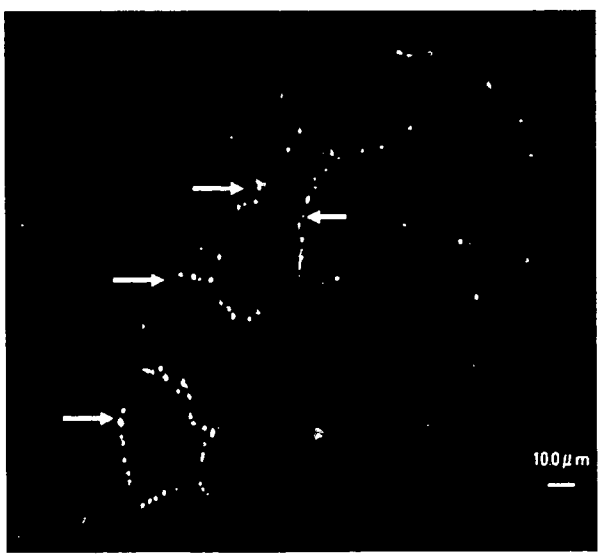

Fig. 1 Confocal laser microscopic image of M1 monolayer cell cultures stained for connexin 43. *Arrows* denote positive connexin 43 staining at the cell-to-cell border of cultured M1 cells. Scale bar = 10 μm

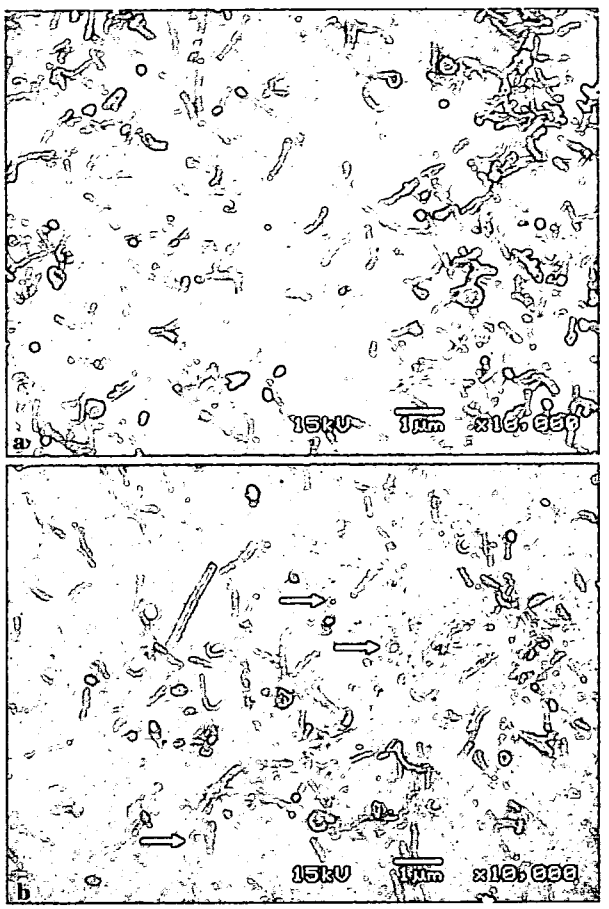

Fig. 2 SEM images of M1 cells in monolayer cell culture conditions. (a) Only a few small pores could be observed on the surface of control M1 cells. (b) An increased number of small pores (*arrows*) resembling coated pits could be observed under IM conditions. Scale bar = 1 μm

Under the combined oleamide/IM treatment conditions, cell-to-cell contact recovered to a large extent (Fig. 3d) and organoid organization was comparable to control conditions (Fig. 3a).

SEM observation of M1 control cells showed small pores (<100 nm) on the surface (Fig. 4a). In IM conditions, besides the presence of small pores, large membrane-bound openings with a diameter size of 200 nm could be routinely detected, indicative of fenestrae (Fig. 4b). On the contrary, oleamide exposure resulted in an almost nonporous surface in M1 cells (Fig. 4c), whereas oleamide administration followed by IM treatment restored the porous aspect of M1 cells as seen after IM treatment alone, i.e., small pores and fenestrae (Fig. 4d).

Discussion

Liver transendothelial transport seems to be a very complex system regulated by numerous structural and molecular pathways which use a variety of signaling molecules, receptors and (cytoskeletal) proteins. Coated pits, vesiculovacuolar organelles, caveolae, micropinocytotic vesicles and fenestrae are all subcellular structural components of the endothelium which play a key role in handling, processing and delivering transendothelial transport cargo from the liver sinusoidal vascular bed to the hepatocytes (Braet & Wisse, 2002). The model of how transport across the liver sinusoidal endothelial barrier is regulated becomes surprisingly even more complicated from this study as we demonstrated that functional GJIC from SEC and/or hepatocytes is able to upregulate or at least to sustain the porosity (area of fenestrae/area of endothelial surface) of M1 SEC cells from a distance (Fig. 4).

This study did not enlighten us about the exact mechanisms by which GJIC regulates fenestral dynamics. However, we hypothesize the following pathway based on our previous and present studies, including the existing literature. In the RFB system, culture medium flows continually, and share stress might influence the structure and function of cells. It is known that share stress changes the cytoskeleton and gene expression and induces cell stretching via connexin 43-mediated autocrine vascular endothelial growth factor (VEGF) secretion (Pimentel et al., 2002; Yamada et al., 2005). Furthermore, it is reported that cAMP levels are increased by IM, which concomitantly enhances GJIC function (Kawasaki et al., 2002). cAMP also induces VEGF gene expression. In line with this, based on the data presented here and preliminary studies, we collected evidence that (1) FLC-5 cells express mRNA of connexins 26, 32 and 43 and connexin 26 is located in the cytoplasm and connexin 32 at the cell rims and (2) M1 cells express mRNA for connexin 43 and are immunoidentified at the cell boundaries. Furthermore, we confirmed the functional integrity of GJIC by the Lucifer yellow assay (*data not shown*). We therefore hypothesize that VEGF secretion is enhanced in FLC-5 cells and acts directly on M1 cells. In addition, it has been reported that VEGF increases fenestral permeability in hepatic sinusoidal endothelial cells (Yokomori et al., 2003; DeLeve et al., 2004) and other sources of vascular endothelium (Roberts & Palade, 1995; Feng et al., 1999; Chen et al., 2002) via paracrine and autocrine pathways. We propose therefore the VEGF-mediated mechanism as one of the plausible mechanisms for the increased vascular permeability observed in the reconstructed liver organoid (Fig. 5).

In conclusion, functional and structural intact GJIC of SECs and/or hepatocytes is able to increase the number of fenestrae in M1-SECs of the liver organoid grown in the RFB coculture system. IM is a promising pharmaceutical compound to be tested first for its beneficial effects on the liver sieve's porosity *in vivo*. This opens up an entire new

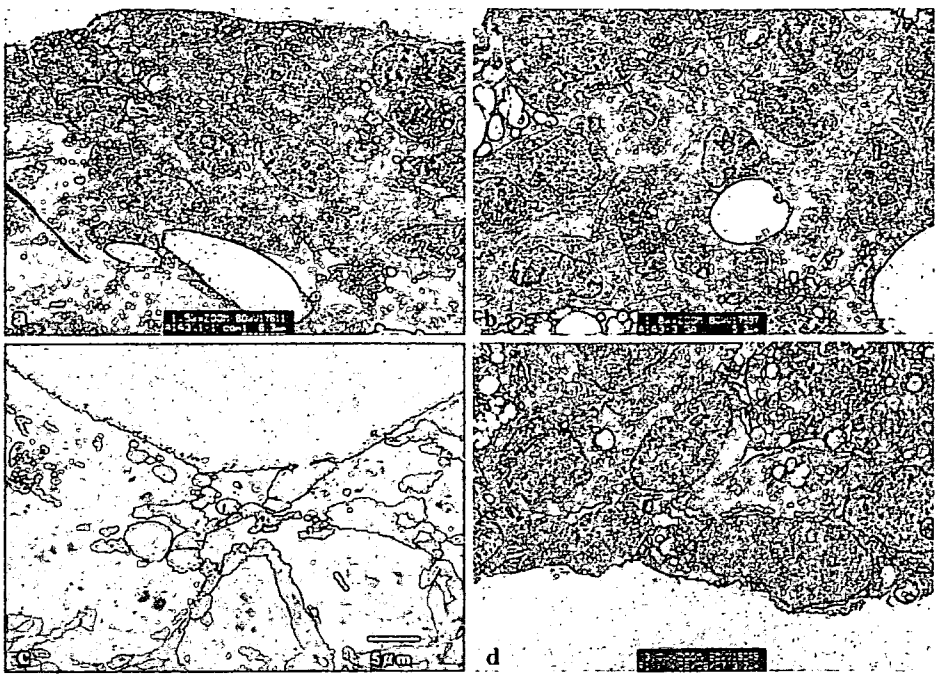

Fig. 3 Low-magnification TEM images of RFB cocultures. (a) TEM observation of control liver organoid shows that cells are organized in multiple layers and interconnected with the neighboring cells, closely resembling liver tissue. Scale bar = 6 μm. (b) IM-exposed RFB cocultures show features similar to those observed under control conditions (*see* a for comparison). Scale bar = 5 μm. (c) Oleamide exposure resulted in a significant decrease in the number of cell-to-cell contacts and, instead, large clefts between the individual cells can be observed. Scale bar = 5 μm. (d) Oleamide followed by IM treatment resulted in restoration of the liver oganoid tissue context. Scale bar = 3 μm

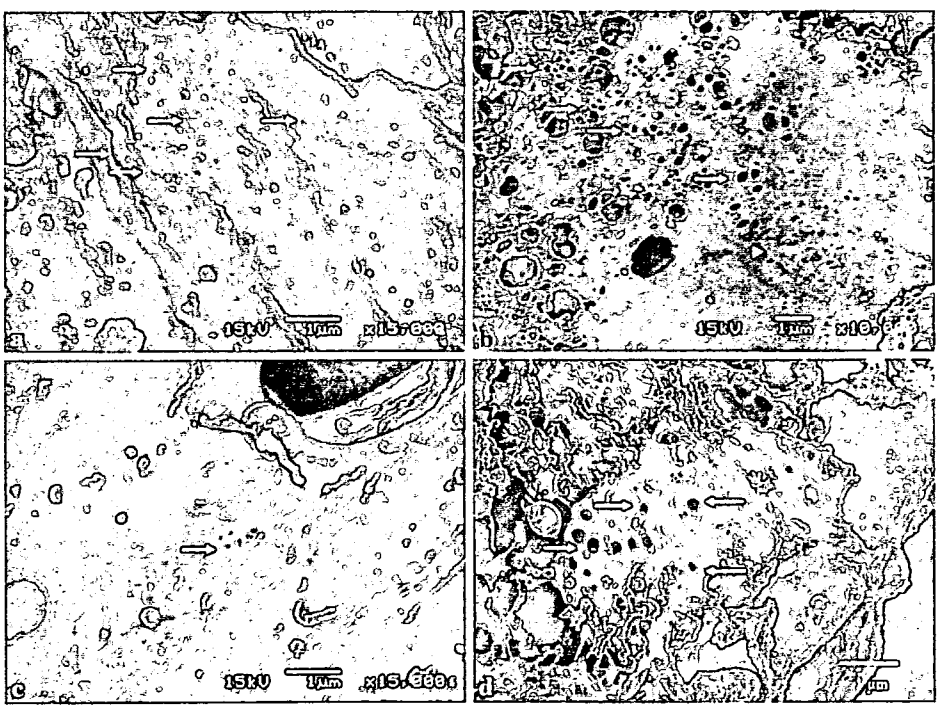

Fig. 4 SEM images of the surface of M1 cells cultured in the RFB system. (a) Small pores (*arrows*) can be observed on the surface of control M1 cells. (b) After IM exposure, small pores (*arrows*) and large openings with a diameter size of 200 nm (fenestrae) and organized in plates could be routinely detected (*arrowhead*). (c) Oleamide treatment resulted in a nonporous appearance of M1 cells. Small pores (*arrow*) could occasionally be observed on the surface of M1 cells. (d) Combined oleamide/IM treatment resulted in the reappearance of the porous surface as observed after IM treatment only (for comparison, *see* b). Scale bars = 1 μm

field in fenestral research in which gap junctions will be targeted, modulated and manipulated in order to restore the liver sieve's porosity or its ability to sieve. The relevant alcohol- or CCl_4-induced defenestration model of cirrhosis in rats in combination with IM and/or oleamide drug treatment might serve as a first step to bridge the gap between the exciting *in vitro* RFB data presented here and the potential future *in vivo* applications.

Acknowledgments T. M. and F. B. acknowledge the support of the Japan Association for the Advancement of Medical Equipment (H17-nano-013 no. 141 from the Ministry of Welfare and Labor of Japan).

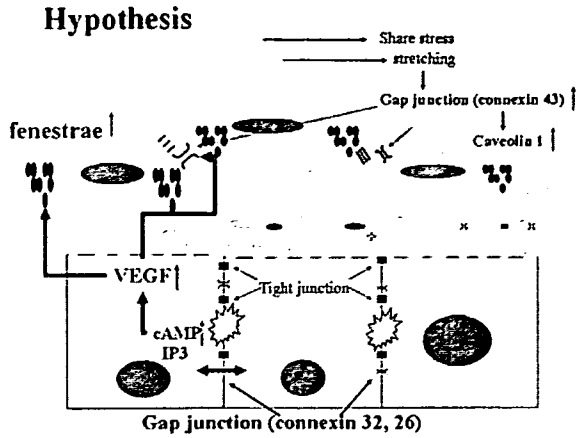

Fig. 5 Schematic presentation of the postulated mechanism by which GJIC might regulate fenestral number in M1 endothelial cells under RFB coculture conditions. As outlined in detail in the Discussion section, the molecules connexin, cAMP and VEGF play a central role in this process. *IP3* inositol 1,4,5-trisphosphate

References

Braet F (2004) How molecular microscopy revealed new insights into the dynamics of hepatic endothelial fenestrae in the past decade. Liver Int 24:532–539

Braet F, Spector I, De Zanger R, Wisse E (1998) A novel structure involved in the formation of liver endothelial cell fenestrae revealed by using the actin inhibitor misakinolide. Proc Natl Acad Sci USA 95:13635–13640

Braet F, Vekemans K, Morselt H, De Zanger R, Wisse E, Scherphof G, Kamps J (2004) The effect of cytochalasin B-loaded liposomes on the ultrastructure of the liver sieve. Comp Hepatol 3(Suppl 1):S27

Braet F, Wisse E (2002) Structural and functional aspects of liver sinusoidal endothelial cell fenestrae: a review. Comp Hepatol 1:1

Braet F, Wisse E, Bomans P, Frederik P, Geerts W, Koster A, Soon L, Ringer S (2007) Contribution of high-resolution correlative imaging techniques in the study of the liver sieve in three-dimensions. Microsc Res Tech 70:230–242

Chen J, Braet F, Brodsky S, Weinstein T, Romanov V, Noiri E, Goligorsky MS (2002) VEGF-induced mobilization of caveolae and increase in permeability of endothelial cells. Am J Physiol 282:C1053–C1063

DeLeve LD, Wang X, Hu L, McCuskey MK, McCuskey RS (2004) Rat liver sinusoidal endothelial cell phenotype is maintained by paracrine and autocrine regulation. Am J Physiol 287:G757–G763

de Wit C, Hoepfl B, Wolfle SE (2006) Endothelial mediators and communication through vascular gap junctions. Biol Chem 387:3–9

Evans WH, Martin PE (2002) Gap junctions: structure and function. Mol Membr Biol 19:121–136

Feng D, Nagy JA, Hipp J, Pyne K, Dvorak HF, Dvorak AM (1997) Reinterpretation of endothelial cell gaps induced by vasoactive mediators in guinea-pig, mouse and rat: many are transcellular pores. J Physiol 504(Pt 3):747–761

Feng D, Nagy JA, Pyne K, Hammel I, Dvorak HF, Dvorak AM (1999) Pathways of macromolecular extravasation across microvascular endothelium in response to VPF/VEGF and other vasoactive mediators. Microcirculation 6:23–44

Fraser R, Dobbs BR, Rogers GW (1995) Lipoproteins and the liver sieve: the role of the fenestrated sinusoidal endothelium in lipoprotein metabolism, atherosclerosis, and cirrhosis. Hepatology 21:863–874

Inoguchi T, Ueda F, Umeda F, Yamashita T, Nawata H (1995) Inhibition of intercellular communication via gap junction in cultured aortic endothelial cells by elevated glucose and phorbol ester. Biochem Biophys Res Commun 208:492–497

Ioannidou S, Deinhardt K, Miotla J, Bradley J, Cheung E, Samuelsson S, Ng YS, Shima DT (2006) An in vitro assay reveals a role for the diaphragm protein PV-1 in endothelial fenestra morphogenesis. Proc Natl Acad Sci USA 103:16770–16775

Jat PS, Noble MD, Ataliotis P, Tanaka Y, Yannoutsos N, Larsen L, Kioussis D (1991) Direct derivation of conditionally immortal cell lines from an H-2Kb-tsA58 transgenic mouse. Proc Natl Acad Sci USA 88:5096–5100

Kawasaki Y, Tsuchida A, Sasaki T, Yamasaki S, Kuwada Y, Murakami M, Chayama K (2002) Irsogladine malate up-regulates gap junctional intercellular communication between pancreatic cancer cells via PKA pathway. Pancreas 25:373–377

Matsuura T, Kawada M, Hasumura S, et al. (1998) High-density culture of immortalized liver endothelial cells in the radial-flow bioreactor in the development of an artificial liver. Int J Artif Organs 21:229–234

Matsuura T, Kawada M, Sujino H, Hasumura S, Nagamori S, Shimizu H (1999) Vitamin A metabolism of immortalized hepatic stellate cell in the bioreactor. In: Cells of the Hepatic Sinusoid, vol 7. The Kupffer Cell Foundation, Leiden The Netherlands, pp 88–89

Nakashima Y, Kohno H, El-Assal ON, Dhar DK, Ueda F, Nagasue N (2000) Irsogladine upregulates expressions of connexin32 and connexin26 in the rat liver. Hepatol Res 18:29–42

Oda M, Han JY, Nakamura M (2000) Endothelial cell dysfunction in microvasculature: relevance to disease processes. Clin Hemorheol Microcirc 23:199–211

Pimentel RC, Yamada KA, Kleber AG, Saffitz JE (2002) Autocrine regulation of myocyte Cx43 expression by VEGF. Circ Res 90:671–677

Roberts WG, Palade GE (1995) Increased microvascular permeability and endothelial fenestration induced by vascular endothelial growth factor. J Cell Sci 108:2369–2379

Rummery NM, Hill CE (2004) Vascular gap junctions and implications for hypertension. Clin Exp Pharmacol Physiol 31:659–667

Saito M, Matsuura T, Masaki T, Maehashi H, Braet F (2004) Study of the reappearance of sieve plate-like pores in immortalized sinusoidal endothelial cells - effect of actin inhibitor in mixed perfusion cultures. Comp Hepatol 3(Suppl 1):S28

Saito M, Matsuura T, Masaki T, Maehashi H, Shimizu K, Hataba Y, Iwahori T, Suzuki T, Braet F (2006) Reconstruction of liver organoid using a bioreactor. World J Gastroenterol 12:1881–1888

Uchida Y, Shiba H, Komatsuzawa H, Hirono C, Ashikaga A, Fujita T, Kawaguchi H, Sugai M, Shiba Y, Kurihara H (2005) Irsogladine maleate influences the response of gap junctional intercellular communication and IL-8 of human gingival epithelial cells following periodontopathogenic bacterial challenge. Biochem Biophys Res Commun 333:502–507

van Veen TA, van Rijen HV, Jongsma HJ (2006) Physiology of cardiovascular gap junctions. Adv Cardiol 42:18–40

Wisse E (1970) An electron microscopic study of the fenestrated endothelial lining of rat liver sinusoids. J Ultrastruct Res 3:125–150

Wisse E, De Zanger RB, Charels K, Van Der Smissen P, McCuskey RS (1985) The liver sieve: considerations concerning the structure and function of endothelial fenestrae, the sinusoidal wall and the space of Disse. Hepatology 5:683–692